

# Detailed Characterization of a Lenster - A mm-wave Flat Lens

Paul Moseley, Giorgio Savini, Elena Saenz, Jin Zhang and Peter Ade

**Abstract** — We perform detailed free-space measurements of a previously published metal-mesh thin, flat gradient index lens using a vector network analyzer. Direct measurements of the transmission and phase of the lens are made over the frequency band of 75–220 GHz, including off axis performance. Beam patterns at 110 and 160 GHz show good agreement with the Airy pattern expectation and demonstrate its relatively broadband performance. We also show that the beam profiles are not affected when it is rotated by  $\pm 6$  degrees with the receiver demonstrating its usability under non-normal illumination.

**Index Terms**—GRIN, Metamaterials, FSS, Lens

## I. INTRODUCTION

A wide range of Frequency Selective Surfaces (FSS) have been designed and created which provide a variety of filter types and specific phase behavior. The first prototype of lenster (lens-filter) was published in 2012 [1] and was the first prototype to demonstrate broadband performance of a frequency selective flat lens at mm wavelengths. Whilst limited measurements of its performance demonstrated the focusing and filtering properties, they did not investigate its broadband antenna pattern characteristics. This paper expands on these measurements by performing detailed beam patterns and 2-D scans on axis, of the transmission and phase of the lens over the frequency range 75 to 220 GHz. This characterizes the frequency dependence of the lens such that it can be compared to the performance of a similar dielectric lens. Details of the lens design can be found in [1] while [2] contains additional details on the underlying metamaterial physics and on the choice of specific parameters of the build.

Other metamaterial flat lenses have been demonstrated using a similar multi-layer approach. They were produced for satellite communication, so were designed to operate at a lower frequency (30 GHz) and have a narrower bandwidth (40%) [3]. There has also been much interest in creating lenses using metasurfaces, which is a single layer metamaterial, that has been designed to operate in the mm-wave to optical frequencies [4]. Due to the inherent properties of the structures used in the

metasurface, the operational bandwidth is limited and they can be highly absorbing due to the resonances in the structures. They also only operate for selected polarisations and orientations, whereas the Lenster is insensitive to polarisation due to symmetrical unit cell structure used. The lens presented in this paper has been designed for astronomical applications, specifically for observing the cosmic microwave background (CMB), as such lenses for this application have to operate over a large bandwidth 50-300 GHz [5]. The only other lens designed for this application that has been demonstrated is given in [6] [7]. This lens was shown to have good transmission properties, but was designed to operate over a narrower band than that presented here.

## II. MODELED LENS PERFORMANCE

For design and simulation purposes, the lens is represented as an ideal material with a continuously varying refractive index [1]. From this the corresponding mechanical structure can be found to mimic the ideal design as closely as possible. This process allows for existing GRIN (Gradient Index) theory to be used as an iterative tool, rather than a potentially much slower parametric simulation process of modelling the entire structure in a finite-element analysis software.

This is a good assumption as the base dielectric used in our designs is polypropylene which has no significant absorption features at frequencies below 13 THz and has a very low absorption coefficient. To determine this and accurately measure the refractive index of polypropylene we have measured the transmission of 9 different hot pressed samples of varying thicknesses between 1 and 8 mm at submillimetre wavelengths using an FT spectrometer. The best fit to the refractive index is  $1.510 \pm 0.005$  and is constant over the measured frequency range. The extracted absorption coefficient is shown in Fig 1 with a polynomial fit, see insert on plot, which is used to extrapolate the absorption to lower frequencies where FT spectroscopic measurements are compromised by the decreasing source power and the low loss in the thickest sample.

Submitted for review 17/11/17. This work was supported by the following grants: Science and Technology Funding Council (STFC) (ST/K00926/1, ST/N000706/1); European Space Agency (ESA) (501100000844 No.4000106146); UCL Impact Scheme.

Moseley & Ade are from School of Physics and Astronomy, The Parade, Cardiff, CF24 3AA ([paul.moseley@astro.cf.ac.uk](mailto:paul.moseley@astro.cf.ac.uk))

Savini is with Optical Science Laboratory, Physics and Astronomy Department, University College London, Gower Street, London WC1E 6BT, UK

Zhang is with Department of Computing and Technology, Faculty of Science and Technology, Anglia Ruskin University, Compass House, 80 Newmarket Road, Cambridge, CB5 8DZ, UK

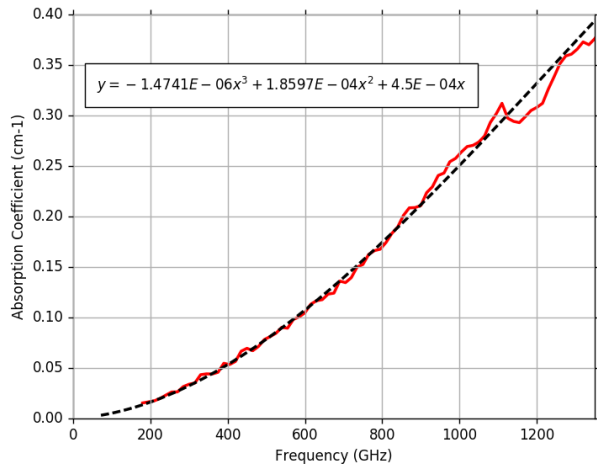


Fig. 1 PP absorption coefficient extracted from transmission measurements of hot pressed layers of thickness between 1 and 8 mm. The polynomial fit is given in the top left corner.

Using this data it can be seen that the expected loss from the lens dielectric substrate, at 2mm thick, is less than 1% at the highest frequency over which the lens is effective, 300GHz. Our lens model uses the bulk electrical conductivity for copper ( $5.80 \cdot 10^7$  mhos/m) with a mesh thickness of 400 nm ( $>$  skin depth 194 nm) and indicates that the mesh absorption is less than 0.1%.

### A. Theory of the Lens Design

The design of the lens is based on a radially graded refractive index lens as first proposed by Wood [9]. The optical properties are defined by (1), which shows how the refractive index,  $n$ , must vary for a given thickness,  $d$ , radius,  $r$ , and focal length,  $f$ .

$$n(r) = n_0 - \frac{r^2}{2df} \quad (1)$$

To be an imaging lens and not just a light collector, the gradient imparted on the lens must satisfy a condition of smoothness for which the variation of index, over the metamaterial unit cell period,  $g$ , is such that,  $\Delta n d/n \ll 1$ , in order to present a smoothly varying phase for the output radiation. It should be noted that there have been other proposed designs for GRIN lenses, either by using transformation optics [10] [11] or by phase transformations [6], [12]. However, these require more complex material parameters, such as a 3-D graded index or anisotropic material parameters. The lens was designed to be similar to a standard polyethylene lens which has a 70 mm diameter and a focal length of 250 mm for comparative purposes. When using the Wood lens formalism, the edge refractive index is constrained by the lowest achievable artificial index, which is set by the index of the substrate, polypropylene,  $n = 1.49$ . Therefore, the maximum index at the center of the lens can be found by rearranging (1) for  $r=35$  mm. With the thickness of the lens chosen to be 2 mm, this makes the index at the center of the lens  $n_0 = 2.7$ . These chosen parameters are based on a trade-off

driven by the underlying mesh structure, as a thinner lens increases the central index value and reduces the number of mesh layers, while increasing the lens does the inverse.

### B. Design Parameters of the Lens

By applying the same metal mesh technology used in astronomical filters [8], it was shown [2] that an artificial dielectric can be created by stacking a number of layers of metal-mesh together with a given uniform spacing. The individual metal-mesh sheets consist of a unit cell size,  $g$ , with a copper patch given by the ratio  $a/g$ . The combined structure is shown in Fig. 2. The effective refractive index is tuned by varying all of these parameters.

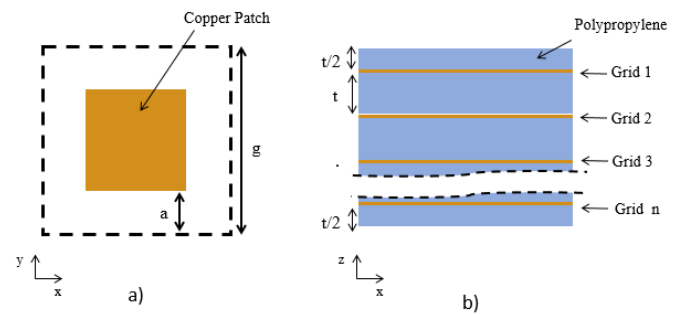


Fig. 2: a) Geometry of a single metal-mesh layer. b) Combined artificial dielectric stack consisting of multiple metal-mesh layers.

By iteratively modelling this basic metal-mesh structure, it was found that a structure of 20 layers with 100  $\mu$ m separation would give the required lens thickness of 2mm [1] whilst being able to achieve a suitable range of refractive indexes by only varying  $a/g$  [2]. The advantage of this is that the cell size is constant at 200  $\mu$ m, which corresponds to a subwavelength size of  $\lambda/7$  for the shortest wavelengths which means that no diffraction effects will occur. The spacing between layers is also constant which simplifies the manufacturing.

### C. Internal Lens Structure

Finite-element modelling of the entire metal-mesh structure of the lens is not currently feasible due to computational limitations. Therefore a reduced model was developed which used symmetry arguments to reduce computations and enable iterations over the design parameters. The model assumes that the impedance over the surface is varying slowly, so that each unit cell appears as an infinite structure [13]. This approximation allows for the existing equivalent-circuit models [14], to simulate the overall transmission properties of the lens by integrating over the entire surface area of the lens to give a power transmission profile. The blue curve in Fig. 3 shows the modelled power transmission for the metamaterial patterns averaged over the lens area. It can be seen that there is about 70% transmission on average, while the remaining 30% of the power is reflection loss due to the miss-match to free space. The models indicate that there is minimal absorption ( $<0.1\%$ ) occurring at these frequencies within the mesh structure and the polypropylene substrate. From here onwards, all references to transmission and reflection correspond to power ratios.

To increase the overall transmission of the lens it is possible to add an anti-reflection coating (ARC) to the lens. For a uniform dielectric the ideal anti-reflection coating on each surface requires an index of  $n_{arc} = \sqrt{n_{sub}}$  and a thickness of  $\lambda / 4n_{arc}$ . In the case of the lens the ARC will also have to be graded following the root of the underlying index profile. This can be achieved by using the same metamaterial approach. It should be noted that to be true to the theory the thickness of the coating should also change which requires a graded metamaterial approach as used in the lens. Here we have set the thickness based on the central index of the lens where the impedance miss-match is the greatest. This coating is simulated in the same way and produces the red curve in Fig.3, which shows nearly 99% transmission at the central design frequency of 150 GHz. To improve the bandwidth of the ARC, a second layer can be added consisting of a uniformly thick sheet of porous PTFE, which has an index of 1.23. When added to the existing ARC, the transmission shown by the green curve is produced, showing that 90% transmission is achieved between 72-250 GHz. Further investigation into more complex multi-layer coatings can be undertaken to optimise the transmission further.

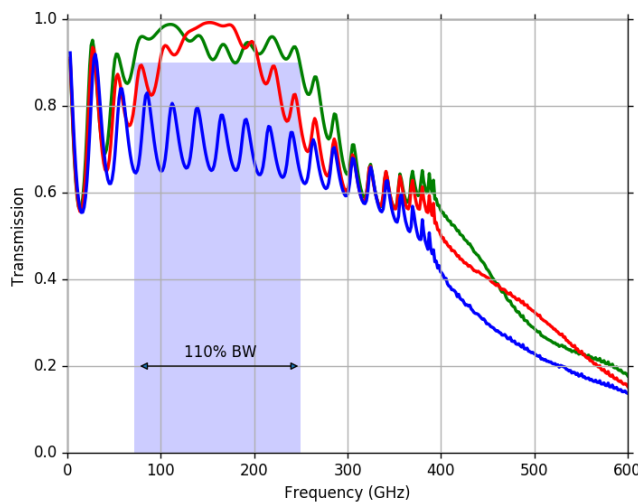


Fig. 3 Predicted power transmission of the uncoated GRIN lens (Blue), the single radially varying ARC coated lens (Red) and combined ARC and porous PTFE coated lens (Green)

#### D. Effective Refractive Index Variation

In the design of the lens, it is assumed that the metal-mesh structure behaves as an ideal bulk material with a constant frequency-independent effective refractive index,  $n$ , regardless of incident angle. In the previous papers [1,2] this was verified using an empirical approach based on modelling the mesh structure in HFSS and then fitting the equivalent ideal dielectric transmission profile. Since the number of mesh layers does not change the equivalent index, it is possible to model an infinite stack and calculate the associated Bloch waves. This was demonstrated in [11], which used an equivalent circuit model to give an analytical expression to calculate the block wavenumber and thus dispersion and bandgap behavior for a stack of patches. From the calculated Bloch wavenumber ( $k_b$ ) the effective index can be found using the relationship given in

equation 2. The effective index profile generated using this approach matches that previous method.

$$n_{eff} = \frac{k_b \lambda}{2\pi d} \quad (2)$$

Using this theoretical relationship, it is possible to calculate how the refractive index distribution deviates from the ideal index values at the central design frequency of 150 GHz and at non-normal incidence for the physical mesh geometry used in the lens.

Results for this study are shown in Fig. 4 which indicates that there is little variation from the ideal index distribution. The maximum bandwidth of the lens is set by the cut-off frequency of the capacitive structure, which for this design is 300 GHz as presented in [1,2].

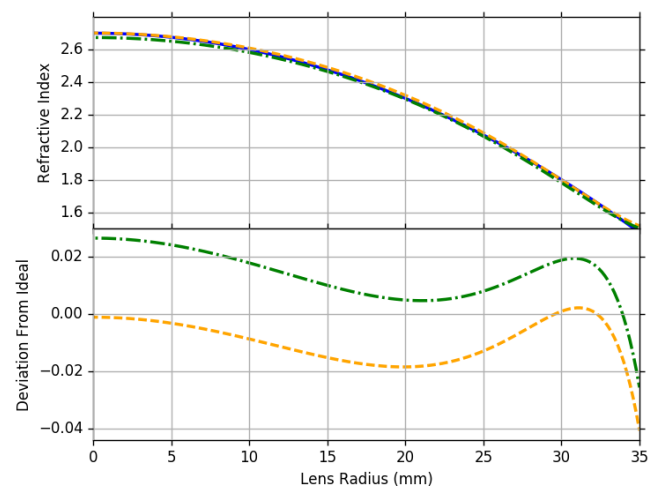


Fig. 4 Deviation in refractive index. Solid blue line: Ideal Woods distribution. Dashed orange line: Realized effective index distribution for 150 GHz at normal incidence. Dash-dotted green line: Realized effective index distribution for 12 degrees incidence.

### III. MEASUREMENT SETUP

To improve on the existing measurements, better knowledge of the phase and transmission characteristics over the full spectral range of the lens are required as well as its directional response. This needs to be measured over an extended volume behind the lens to examine the near focus of the lens and thus to explore any aberrations. To get the desired spectral resolution a vector network analyzer (VNA) was used in conjunction with a set of three frequency extenders to cover the bands 75–110 GHz, 110–170 GHz and 170–220 GHz. This coherent setup allows for direct measurements of the phase. A diagram showing the measurement configuration, along with the associated axis, is given in Fig. 5.

The lens was illuminated with a plane wave with constant phase across its aperture. This was achieved by using the quasi-optical bench at ESA/ESTEC [15]. This consists of an ellipsoidal mirror which shapes the beam such that the beam waist at the lens position is by approximated a uniform plane wave. The receiver head is placed on moveable stage in the lens focal plane to map out the pattern as described below.

### A. Normal Incidence Configuration

To scan the beam pattern both in angle and through the focus, the receiver was placed on an adjustable 2-D stage that allowed for precise positioning with an accuracy of 0.1 mm in the x-y plane. This stage was itself attached to a manually adjustable linear translator for motion along the z-axis with a positional accuracy of <1 mm. Since the lens is radially symmetric, a full 3-D sampling was not required, instead 2-D slices across the optical axis were taken for a set of incremental steps along the z-axis covering the focal region. For these measurements, it was crucial for the optical axis of the lens to be parallel to the optical table plane and coincident with the receiver horn axis. In addition the transverse scans had to be parallel to the lens plane. Any misalignments of the optics would affect the phase front measurement. To align the axes, a series of phase measurements without the lens in place were made. Since the measured phase should be constant, any misalignment between the transmitter, ellipsoidal lens and receiver optical axes would appear as a slope in the data. From the direction of the slope, adjustments to the scanner position were made and checked iteratively until the phase is flat.

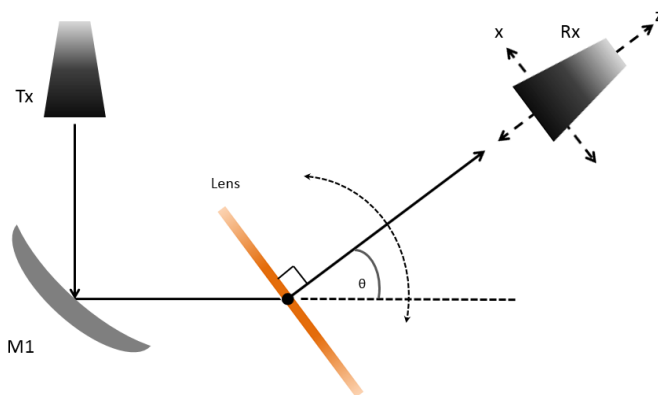


Fig. 5 Illustration of the experimental setup. M1 is an ellipsoidal mirror that collimates the beam such that a plane wave is approximated at the lens position. For the normal incidence measurement,  $\theta$  is fixed at zero. The receiver is scanned in the x and z directions (y is vertical to the plane of the bench). For the beam pattern measurements, the position of the receiver in x and z is fixed while  $\theta$  is varied. The lens plane is orthogonal to the receiver axis.

### B. Oblique Incidence Configuration

In practical applications the lens needs to operate over a range of incidence angles. To investigate how the lens behaves under off-axis illumination we have measured the beam profile by rotating both the lens and receiver head as a fixed unit about the

collimated beam axis, as shown in Fig. 6. A fixed laser system, in which the laser was reflected off a mirror mounted at the centre of rotation of the lens, allowed the deflection angle to be determined by measuring the position of the reflected spot on a screen at a known distance. For these measurements the 110–170 GHz receiver was used and a scan range of  $\pm 6$  degrees was sufficient to cover the beam profile expected.

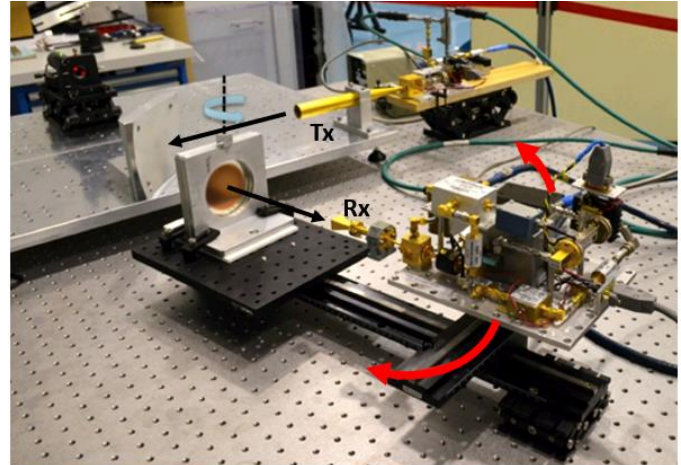


Fig. 6 Beam pattern measurement setup. The receiver (Rx) can pivot around the centre of the lens in an arc defined by the red arrows.

## IV. MEASUREMENTS, RESULTS AND DISCUSSIONS

To explore the beam focus region a set of measurements were taken of through-focus x-axis beam cuts at the vertical beam center as a function of z-axis position as described in III A. The beam was sampled in 1 mm intervals along the x-axis and 5mm intervals in z. These sparsely populated cuts were then interpolated to produce a graded intensity profile as shown in Fig. 7 for an input frequency of 150 GHz at normal incidence. The beam waist narrows around the focus of the lens at  $z = 230$  mm. For comparison the same scan was repeated without a lens in place to show the level and uniformity of the field.

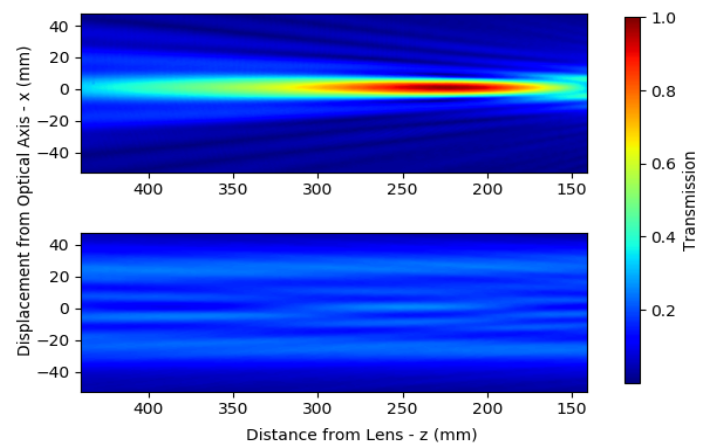


Fig. 7 Top: Interpolated 2-D field scan at 150 GHz, showing that the lens focus is at the distance of 230 mm. Bottom: Measured field without the lens in place.

The size of the beam waist is comparable to that expected of a diffraction-limited dielectric lens of the same diameter and focal length. Fig. 8 shows an x-cut through the focus of the Lenster (Blue curve) and the clear aperture (Green) from Fig. 7. We also repeated the measurement with a polyethylene lens and plot the focus x-cut (Orange) on the same scale. Unfortunately an equivalent polyethylene lens was not available, so a lens with 80mm diameter and 180 mm focal length was used. The apparent increase in gain of the polyethylene lens over the Lenster is due to its larger collecting area. To accurately compare the two lenses the overall transmission efficiency for each can be used. This was calculated by first integrating over the incident aperture field and then integrating over the airy profile at the focus. These two quantities can then be ratioed to give the lens efficiency. For an ideal system all the power incident on the lens is focused into the airy pattern. Therefore, any reflections due to the lens will cause a decrease. The measured optical efficiency in a 10 GHz band centered at 150 GHz is  $87.9\% \pm 3.5\%$  for the polyethylene lens and  $75.0\% \pm 3.2\%$  for the GRIN lens. The efficiency of polyethylene lens matches the averaged reflective loss for a material with refractive index of 1.51. The GRIN efficiency is lower as expected due to the higher refractive index at the centre of the lens. However, the measured value is comparable to the predicted transmission shown in Fig 2, indicating that as expected the absorption losses are small.

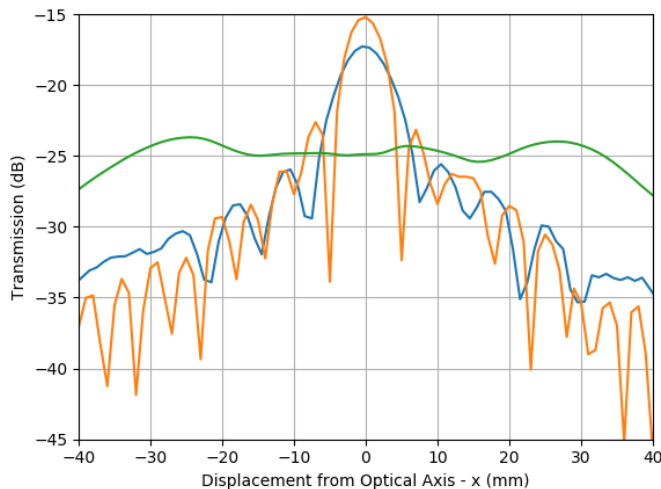


Fig. 8: x-axis beam cuts at 150GHz comparing the GRIN lens (Blue) and Polyethylene lens (Orange) at their optimal focus. The measured x-cut with no lens is shown in Green. The dielectric lens has a larger diameter and shorter focal length.

Comparisons of the measured beam profiles to the Airy diffraction model for measurements made at the correct focus position for frequencies of 116 and 290 GHz are also shown in Fig. 9. The Airy model, given by the solid curves, fits the data points for the main beam and follows the predicted behavior of the side lobes. Since it is not possible to eliminate all of the scattered power, the side lobe measurements below -25 dB are

contaminated by standing-wave residuals.

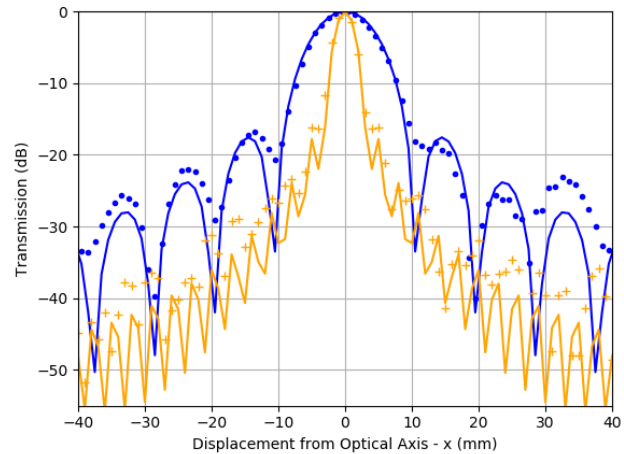


Fig. 9. x-axis beam cuts, at the nominal focus position of 230mm, for 116 GHz blue dots and 290GHz orange cross. The expected Airy profiles for each are shown as continuous lines.

Fig. 10 shows the measured phase for beam cuts about the optical axis as a function of z-axis position for a frequency of 100 GHz. We expect the phase to be flat at the focus albeit with a slope which would be indicative of small misalignments. The data in Fig. 10 indicates that the flattest phase is at 230 mm with a slope indicating that there was some misalignment. These data are in agreement with those presented in Figures 7 and 8.

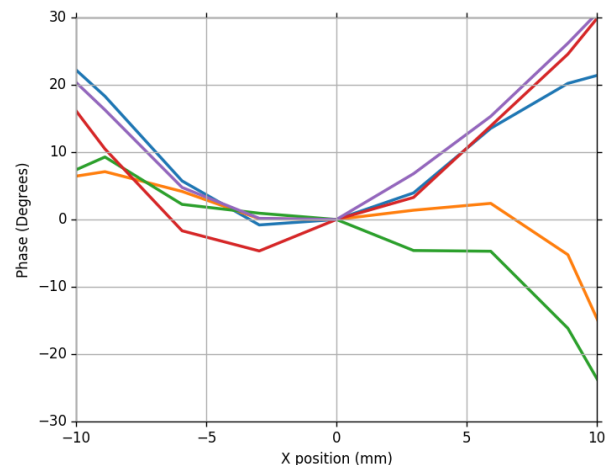


Fig. 10 The phase variation across the lens at 100 GHz as a function of z-axis position. From top to bottom at left-most extreme, Blue: 310 mm, Purple: 150 mm, Red: 190 mm, Green: 230 mm, Orange: 250 mm.

To explore the performance under non-normal illumination the beam profile was measured at four different frequencies while rotating the lens and receiver by  $\pm 6$  degrees about the collimated beam input axis as described in III.B. Fig 11 shows that the main beam is well defined and closely matches the Airy expectation down to -17 dB. This result is important as it clearly demonstrates that the properties of the metamaterial used here do not change under off-axis illumination unlike some more

exotic metamaterials [16]. Again we note with hindsight that the lack of absorbing material to control systematics prevented a clear measurement of the side lobes.

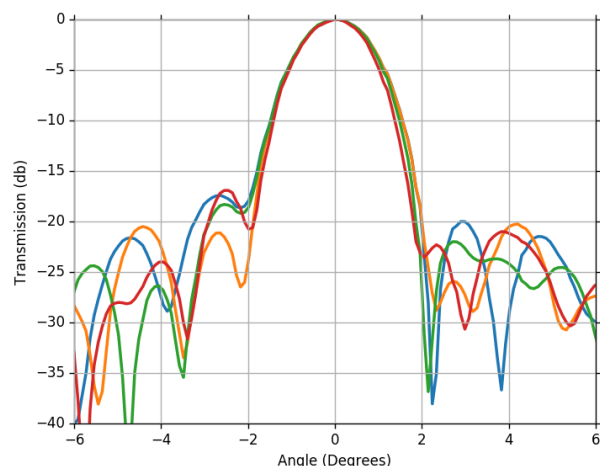


Fig. 11 Beam pattern measurements of the lens for multiple frequencies. Blue: 130 GHz, Orange: 140 GHz, Green: 150 GHz, Red: 160 GHz. Plots have been normalized to the peak for clarity.

## V. CONCLUSION

We have shown that a GRIN lens is a viable alternative to standard dielectric lenses currently used in THz instrumentation. The prototype described here is usable over a wide frequency band 80-290 GHz and experimentally shown to operate at 116-290 GHz. From an instrumental usage point of view it also has the advantage that it behaves as a low pass filter reflecting incident higher frequencies. These properties will prove valuable in future cryogenic receivers.

The advantage of such a component over a normal lens becomes apparent when larger diameter short focal length lenses are required. Whereas the thickness of a large-diameter GRIN lens will not increase significantly with size, the corresponding dielectric lens will become much thicker to accommodate the curvature radius of its surfaces. Since the absorption of a thick polyethylene (a standard millimeter wave material) substrate increases significantly with frequency, this limits the usable spectral range for such lenses. With our GRIN lens, the material is much thinner so scaling to THz frequencies is possible. Further, the addition of index graded anti-reflection coatings would be easier to apply to the flat GRIN lens and would enhance its overall transmission and efficiency.

## REFERENCES

- [1] G. Savini, P. A. R. Ade and J. Zhang, "A new artificial material approach for flat THz frequency lenses," *Opt. Express*, vol. 20, pp. 25766-25773, Nov 2012.
- [2] J. Zhang, P. A. R. Ade, P. Mauskopf, L. Monceli, G. Savini and N. Whitehouse, "New artificial dielectric metamaterial and its application as a terahertz antireflection coating," *Appl. Opt.*, vol. 48, pp. 6635-6642, Dec 2009.
- [3] M. & B. N. Li, "Wideband true-time-delay microwave lenses based on metallo-dielectric and all-dielectric lowpass frequency selective surfaces," *IEEE Trans. Antennas Propag.*, vol. 61, no. 8, pp. 4109-4119, 2013.
- [4] N. Y. a. F. Capasso, "Flat optics with designer metasurfaces," *Nat. Mater.*, vol. 13, no. 2, pp. 139-150, 2014.
- [5] M. H. e. a. Abitbol, CMB-S4 technology book, 2017.
- [6] G. Pisano, M. W. Ng, F. Ozturk, B. Maffei and V. Haynes, "Dielectrically embedded flat mesh lens for millimeter waves applications," *Appl. Opt.*, vol. 52, pp. 2218-2225, Apr 2013.
- [7] A. S. P. M. C. T. G. S. P. A. Giampaolo Pisano, "Development of large-diameter flat mesh-lenses for millimetre wave instrumentation," in *Proc. SPIE 10708, Millimeter, Submillimeter, and Far-Infrared Detectors and Instrumentation for Astronomy IX*, Austin, 2018.
- [8] P. Ade, G. Pisano, C. Tucker and S. Weaver, "A review of metal mesh filters," in *Society of Photo-Optical Instrumentation Engineers (SPIE) Conference Series*, 2006.
- [9] J. B. Caldwell, "Optical design with Wood lenses 1: infinite conjugate systems," *Appl. Opt.*, vol. 31, pp. 2317-2325, May 1992.
- [10] J. B. Pendry, "Negative Refraction Makes a Perfect Lens," *Phys. Rev. Lett.*, vol. 85, no. 18, pp. 3966-3969, Oct 2000.
- [11] C. Mateo-Segura, A. Dyke, H. Dyke, S. Haq and Y. Hao, "Flat Luneburg Lens via Transformation Optics for Directive Antenna Applications," *Antennas and Propagation, IEEE Transactions on*, vol. 62, pp. 1945-1953, April 2014.
- [12] S. Jain, M. Abdel-Mageed and R. Mittra, "Flat-Lens Design Using Field Transformation and Its Comparison With Those Based on Transformation Optics and Ray Optics," *Antennas and Wireless Propagation Letters, IEEE*, vol. 12, pp. 777-780, 2013.
- [13] S. Maci, M. Caiazzo, A. Cucini and M. Casaletti, "A pole-zero matching method for EBG surfaces composed of a dipole FSS printed on a grounded dielectric slab," *Antennas and Propagation, IEEE Transactions on*, vol. 53, pp. 70-81, Jan 2005.
- [14] S.-W. Lee, G. Zarrillo and C.-L. Law, "Simple formulas for transmission through periodic metal grids or plates," *Antennas and Propagation, IEEE Transactions on*, vol. 30, pp. 904-909, sep 1982.
- [15] ESA. [Online]. Available: [http://esamultimedia.esa.int/docs/space\\_engineering/Material\\_RF\\_characterisation\\_Facilities.pdf](http://esamultimedia.esa.int/docs/space_engineering/Material_RF_characterisation_Facilities.pdf).
- [16] F. e. a. Aieta, "Multiwavelength achromatic metasurfaces by dispersive phase compensation.," *Science*, vol. 347, no. 6228, pp. 1342-1345, 2015.
- [17] C. S. R. Kaipa, A. B. Yakovlev, F. Medina and F. Mesa, "Transmission through stacked 2D periodic distributions

of square conducting patches," *Journal of Applied Physics*, vol. 112, pp. -, 2012.

- [18] G. N. M. W. O. F. M. B. & H. V. Pisano, "Dielectrically embedded flat mesh lens for millimeter waves applications.," *Applied optics*, vol. 52, no. 11, pp. 2218-2225, 2013.



**Paul Moseley** was born in Redditch, United Kingdom in 1988. He received his MPhys degree in physics from Cardiff University, Wales 2011. He received as PhD in physics and astronomy from University College London in 2014. Since then he has been working as a postdoctoral research associate in the astronomy instrumentation group at

Cardiff University. His research interests including designing novel meta-material devices for sub-millimeter and far infrared instruments.

Dr Moseley was made a scholar by the worshipful company of scientific instrument makers for his PhD research.



**G Savini**, received Masters and PhD from Rome University "La Sapienza" in 2001 and 2005 respectively. As post-doctoral research associate he worked from 2004 to 2008 in Cardiff University on far-infrared optics including filters, lenses and polarization modulators. He worked on the calibration and testing of the Planck High Frequency Instrument and software pipeline validation

for the FTS spectrometer on the Herschel Space Observatory. From 2009 he was Lecturer and then Reader in 2013 in the Physics and Astronomy Dept. at University College London. There in the Optical Science Laboratory Dr Savini researches mainly on far-infrared optics and instrumentation design and modelling. Since 2015 he is also the Director of the University College London Observatory with a focus on undergraduate Teaching and Science Outreach.



**Elena Saenz** (S'04–M'08) was born in Viana, Navarra, Spain, in 1981. She received the M.Sc. and Ph.D. degrees from the Public University of Navarra (UPNA), Pamplona, Spain, in 2004 and 2008, respectively, both in telecommunication engineering. Until 2008, she was with the Antenna Group, Public University of Navarra. Since then, she has been working

with the European Space Research and Technology Centre (ESTEC), European Space Agency (ESA), Noordwijk, The Netherlands, with main interest in frequency/polarization

selective surfaces, (sub)millimeter wave technologies, antenna measurements and material characterization.

Dr. Saenz was the recipient of the Loughborough Antennas and Propagation Conference (LAPC) 2006 and 2007 Best Paper Awards, the International Workshop on Antenna Technology (IWAT) 2007 Best Paper Award, and the IEEE Antennas and Propagation Society Graduate Research Award in 2008.



**Jin Zhang** received the PhD degree in 2007 from the Faculty of Computing, Engineering and Science, University of South Wales, UK. She is currently serving as a senior lecturer in Computing & Technology Department in the Anglia Ruskin University. Prior to this she served

as a PDRA in Astronomical Instrumentation Group in Astronomy & Physics Department, Cardiff University, UK. She has intensive research interest in electronic systems modelling, smart antennas, the study and design for development of novel artificial metamaterials components in the mid-infrared range and lower spectral range. The design of quasi-optical components for millimetre-wave astronomy. The electromagnetic modelling and the simulations. She has published over 32 research articles and 8 refereed papers. Was responsible for two Royal Society China-UK Science Network Grants in 2008 and 2009 on behalf of the UK Government Office for Science (GO-Science) and by the China Scholarship Council (CSC) on behalf of the Ministry of Education in China.



**P A R Ade**, received BSc degree in Physics and his PhD from Queen Mary College, University of London, in 1969 and 1973 respectively.

From 1973 to 1976 he held a Science Research Council Fellowship and held a post at national Radio Astronomy Observatory in Tucson on the development of bolometric receivers for sub-millimeter astronomy. In 1976 he was appointed a lecturer at Queen Mary College and was promoted to a Reader in 1986 and then a Professor in 1994. In 2001 he moved his research group to the School of Physics and Astronomy at Cardiff University. Professor Ade has worked on several astronomical satellite instruments (ISO, Cassini, Spitzer, Planck-HFI, and Herschel-Spire) and many sub-orbital instruments at submillimeter wavelengths. His work has been centered on the development of detectors and quasi-optical components at submillimeter wavelengths.

Professor Ade has received the Jackson Gwilt medal from the royal Astronomical Society and a Public Service Medal from NASA.